EUROPEAN RESPIRATORY *journal*

FLAGSHIP SCIENTIFIC JOURNAL OF ERS

Early View

Original Research Article

Deep brain stimulation of the motor thalamus relieves experimentally induced air hunger

Tom p Chapman, Amir p Divanbeighi Zand, Emmanuel Debrah, Beth Petric, Sarah M Farrell, James J FitzGerald, Shakeeb H Moosavi, Alexander L Green

Please cite this article as: Chapman Tp, Divanbeighi Zand Ap, Debrah E, *et al*. Deep brain stimulation of the motor thalamus relieves experimentally induced air hunger. *Eur Respir J* 2024; in press (https://doi.org/10.1183/13993003.01156-2024).

This manuscript has recently been accepted for publication in the *European Respiratory Journal*. It is published here in its accepted form prior to copyediting and typesetting by our production team. After these production processes are complete and the authors have approved the resulting proofs, the article will move to the latest issue of the ERJ online.

DEEP BRAIN STIMULATION OF THE MOTOR THALAMUS RELIEVES EXPERIMENTALLY INDUCED AIR HUNGER.

Tom P Chapman[1,2], Amir P Divanbeighi Zand[2,3], Emmanuel Debrah[2], Beth Petric[2], Sarah M Farrell[2,3] , James J FitzGerald[2,3], Shakeeb H Moosavi[1,2], Alexander L Green[2,3]

[1]Department of Biological and Medical Sciences, Oxford Brookes University, Headington, UK.
[2] Department of Clinical Neurosciences, John Radcliffe Hospital, Oxford, UK.
[3] Nuffield Department of Surgical Sciences, University of Oxford, UK.

Corresponding Author:

Shakeeb H Moosavi

Reader in Clinical Physiology

Department of Biological and Medical Sciences

Faculty of Health and Life Sciences

Oxford Brookes University

Room SNC3.06, Sinclair Building

Gipsy Lane, Oxford OX3 0BP

email: smoosavi@brookes.ac.uk

Take home message: DBS of the motor thalamus using stimulus parameters that are optimal for tremor relief, provides significant relief of experimentally induced hypercapnic air hunger. This advances our understanding of the cerebral mechanisms of breathlessness.

ABSTRACT

Research question: We previously reported that Deep Brain Stimulation (DBS) of motor thalamus (MT), in a patient with post-stroke tremor, relieved breathlessness associated with chronic obstructive pulmonary disease. This raised the question of whether MT DBS mitigates the ascending dyspnoea signal. We therefore sought to conduct a fully powered cohort study of experimentally induced air hunger (AH), an uncomfortable urge to breathe in patients with MT DBS ON and OFF.

Methods: 16 patients (3 females) with DBS of the ventral intermediate nucleus (VIM) as treatment for tremor, underwent hypercapnic AH tests, with DBS 'ON' and 'OFF'. Patients rated AH on a visual analogue scale (VAS) every 15s. Hypercapnia and ventilation were matched for ON and OFF states (mean±sd 43±4 and 43±4mmHg for end-tidal PCO_2, 13.7 and 13.4 L/min for ventilation). Participants ventilation was constrained to baseline levels by breathing from a 3-litre inspiratory reservoir with fixed flow of fresh gas while targeting their resting breathing frequency to a metronome.

Results: Overall steady state AH was 52±28%VAS for 'ON' and 67±20%VAS for 'OFF' (p=0.002; two-tailed paired t-test). The mean reduction in AH during VIM DBS was -14.4%VAS. MT DBS relieved AH in thirteen patients, heightened AH in two and caused no change in one.

Conclusion: MT DBS for tremor relief also mitigates the AH component of dyspnoea. We posit that DBS of the MT heightens the gating control of the thalamus modulating the ascending air hunger signal. Extent of relief suggests that thalamic DBS may prove to be a viable therapy for intractable dyspnoea.

INTRODUCTION

Dyspnoea, defined as “a subjective experience of breathing discomfort” that is prevalent across multiple conditions[1], severely impacts quality of life[2] which may reflect a sparsity of safe and effective treatments. A comprehensive understanding of the central neurophysiology of dyspnoea will help to discover targeted therapies. This approach is facilitated by several advances: a) Distinct components of breathlessness, encapsulated by ‘air hunger’ (AH), ‘sense of breathing effort’, and ‘chest tightness’, have been characterised that can vary independently[3]. b) Different neural mechanisms have been postulated for the different components[4]. c) Methods have been established to induce specific components in experimental settings[5]. AH, defined as an “uncomfortable urge to breathe”, can be induced by raising inspired CO_2 while constraining ventilation; thereby providing a reliable experimental model of a particularly unpleasant component of pathological breathlessness[6].

Cerebral mechanisms have been studied primarily using brain-imaging of experimentally-induced breathlessness in healthy individuals. Experimental AH, and breathlessness associated with resistive loading, have both elicited strong activation of the insular cortex[7-12] with consistent activation of other regions such as anterior cingulate, orbitofrontal cortex, thalamus, amygdala, and basal ganglia have also been implicated in the above studies. How these different areas function as a network for dyspnoea perception is yet to be unravelled.

Deep brain stimulation (DBS), involving implanted electrodes providing constant electrical stimulation of specific brain regions, is a therapy for various neurological conditions including movement disorders, and intractable pain[13]. Several of the DBS sites coincidentally overlap with areas identified in brain-imaging studies of dyspnoea[7] thus offering an alternative approach to investigate cerebral mechanisms.

We previously reported AH relief during DBS of the motor thalamus (ventral intermediate nucleus, VIM), in an individual with post-stroke tremor who coincidentally had pre-existing breathlessness from COPD[14]. The thalamus mirrors phrenic nerve firing, representing the drive to breath once a certain threshold is reached[15]. One hypothesis that follows is that the AH signal, generated by the mismatch between brainstem respiratory corollary discharge and vagal afferents from the lungs, projects to the thalamus whereby a dyspnoea signal is distributed to cortical sensory areas. Here, we hypothesised that DBS of the VIM would mitigate experimentally induced AH, raising the possibility that this region could be a target for relief of intractable dyspnoea by neuromodulation.

METHODS

Participants

Sixteen patients who underwent DBS of the bilateral VIM to treat chronic tremor were recruited consecutively from a single centre at John Radcliffe Hospital, Oxford, UK. All participants provided written informed consent. Ethical approval was provided by South Central Oxford REC (11/SC/0229). The trial was registered on Clinicaltrials.gov (NCT04058457). Eligibility criteria included individuals over the age of 18 who have DBS of the VIM. Exclusion criteria included; females who are pregnant, subjects participating in a clinical investigation that includes an active treatment arm which may affect the respiratory system, and indication of acute respiratory problems at the time of the experimental session.

Sample size

Previous studies involving experimentally induced AH rated on a visual analogue scale (VAS) by healthy volunteers showed a linear increase in VAS ratings of AH with a slope of 6.7%VAS for every 1mmHg rise in end-tidal $P\text{CO}_2$ ($P_{ET}CO_2$) above normocapnia (40mmHg). The standard deviation (SD) of this response slope was 2.4%VAS/mmHg[16]. From this data we determined that an increase in $P_{ET}CO_2$ to 47.5mmHg would produce a mean AH rating of 50%VAS with a SD of ±19%VAS. The minimal clinically important difference (MCID) for VAS ratings of AH is estimated to be between 10-20mmVAS[17, 18]. We chose 15% as this lies in the middle of this range to determine the number of participants we would need as a result of a change of this magnitude to be definitive. Assuming a true difference of ±15%VAS in the mean VAS rating of AH at this level of hypercapnia between DBS OFF versus ON, which is above the minimal clinically important difference of ±10%VAS for breathlessness ratings using VAS, we determined that we would need to study 16 patients to be able to reject the null hypothesis with 85% power and a Type I error probability of 0.05 (PS v3, URL: http://biostat.mc.vanderbilt.edu/PowerSampleSize).

Experimentally-induced air hunger

Participants sat semi-reclined in a comfortable chair. They breathed through a mouthpiece connected via a bacterial filter to a pneumotachograph. The airflow signal was electronically integrated to provide online tidal volume (FV156 respiratory flow integrator, Validyne Engineering Corp, CA, USA). A fast-responding gas analyser (ML206, AD instruments, Oxford, UK) was used to measure breath-by-breath expired CO_2 via a sample line inserted into the mouthpiece. A second sample line inserted in the mouthpiece was connected to a differential pressure transducer (DP45, ±50cmH_20, Validyne Engineering Corp, CA, USA) for continuous measurement of airway pressure. One-way breathing valves (Hans Rudolph, Kansas, USA) separated inspiration from expiration. A 3-litre anaesthetic bag provided the inspiratory reservoir.

A fixed flow of heated and humidified air (HC150 humidifier, Fisher & Paykel Healthcare, NZ) was fed into this bag. Participants breathed to a metronome with a beep-rate set to match the participant's resting spontaneous breathing frequency. To induce AH, up to 7%CO_2 was added to the inspiratory reserve using an air-oxygen blender (Inspiration Health, Croydon, UK) to which gas cylinders containing 10% CO_2 in air, and medical air were connected. Flow of fresh gas to the inspiratory reserve was kept constant and set to match the participants' spontaneous resting ventilation. Participants rated their AH using a slider to operate an electronic 100mm visual analogue scale (VAS). Ratings were cued by an LED that lit every 15s (figure 1A). Arterial oxygen saturation was measured using a finger-pulse oximeter. Blood pressure was measured every 2-3 minutes using the oscillatory cuff method and ECG using 6-lead cutaneous AgCL electrodes.

Protocol

Participants completed three practice 'ramp' tests involving 1-min increments in inspired CO_2. For the first ramp, participants rated 'any breathing discomfort'. Subsequently, a debrief questionnaire[19] involving volunteered comments followed by patient selection of respiratory and non-respiratory descriptors from pre-set lists, was used to ensure participants could differentiate AH from other sensations. Participants were then instructed to solely focus on, and rate AH, during subsequent testing. Two steady-state (SS) AH tests were then completed which involved a sustained increase in inspired CO_2 for 5-min at a level targeting the $P_{ET}CO_2$ associated with AH ratings approximating 50%VAS during initial ramp tests. The order of ON and OFF DBS was randomised between SS tests (figure 1B). End-point was when tolerance was reached, participants came off the mouthpiece, or $P_{ET}CO_2$ reached 60mmHg.

Figure 1 here

Data processing and analysis

Analogue signals were digitised (Micro1401, Cambridge Electronic Design, Cambridge, UK) at a sample rate of 20Hz and stored for offline analysis using Spike2 software (v10, Cambridge Electronic Design, Cambridge, UK). VAS ratings of AH and breath-by-breath $P_{ET}CO_2$ were derived by peak-detection (Spike2).

Shapiro-Wilks test was used to check if the data were normally distributed. Given that this was the case, a two-tailed paired Student's t-test was performed to compare average AH ratings in the last minute of SS between DBS ON and OFF conditions. This region of interest (ROI) took place 15 minutes after switching ON or OFF DBS to allow for stabilisation of the patient's tremor. Figure 2 shows a sample physiological trace of the practice ramp(A) and SS tests (B). The green box represents the region of interest where data were averaged and analysed.

Figure 2 here

Brain imaging

Lead-DBS V3[20], an electrophysiologically validated processing and analysis pipeline, was used to localise and visualise electrodes. One patient data set was excluded (011) as the subject had unilateral electrodes and this process requires bilateral electrodes. Pre-operative T1 MRI and post-operative CT scans were co-registered using a two-stage linear registration (rigid followed by affine) as implemented in Advanced Normalisation Tools (ANT's)[21]. Electrode localisations were corrected for brainshift in postoperative acquisitions by applying a refined affine transform calculated between pre- and postoperative acquisitions that were restricted to a subcortical area of interest. Pre- and post-operative acquisitions were spatially normalised into MNI152NLin2009Asym space (MNI152)[22] using symmetric diffeomorphic image registration (SyN) implemented in ANT's.

Electrode models were selected and automatically pre-localized in native & template space using the PaCER algorithm[23]. If these failed to accurately localise electrodes, tips and trajectories were manually processed within a user interface in Lead-DBS. Orientation of directional DBS leads was determined using the algorithm published by Dembek et al. 2021[24].

Electrodes were then manually localized based on post-operative acquisitions using a tool specifically designed for this task, rendered in template space (MNI152) using a template to define regions of interest, in this case the DISTAL-medium atlas defining subdivisions of the thalamus[25]. Post-operative CT scans were also checked against the electrode positioning in template space. Lead-group[26] was then used to group electrode localisations in template space. (Figure 3A). Amplitudes were inputted for each electrode in each hemisphere, and active contacts selected (Figure 3B). AH responses were then correlated with active contact positionings(Figure 3C).

To verify within-subject and MNI space registration accuracy of the LeadDBS model, individual electrode reconstructions were performed in subjects' native space in a parallel, confirmatory analysis. Postoperative CT images were registered to subjects' T1-weighted preoperative MR series using FMRIB's Linear Image Registration Tool (FLIRT)[27, 28] as implemented in the FMRIB Software Library (FSL) version 6.0.7.10[29]. Active contacts were reconstructed from known electrode geometry and CT artefacts in subjects' native space. The FSL FIRST toolbox[30] was utilised to provide individual model-based segmentation of each subject's thalamus, applying recommended boundary-correction settings; grey-white matter segmentation using FSL FAST (FMRIBS Automated Segmentation Tool).

RESULTS

Participants

Thirty six patients with DBS of the VIM were approached to take part in this study. Thirty patients were eligible with nine declining participation. Five patients were unable to complete the AH test due to their tremor severity during OFF DBS. Sixteen patients (3 female) with essential (n=11), dystonic (n=2), both essential and dystonic (n=1) and Parkinsonian tremor (n=2), were studied between 12/09/2019 (date first patient was studied) and 27/06/2023 (date last patient was studied). Mean±sd age, height and weight were 66±10yr, 174±8cm, and 182±26lbs (Table 1). Electrodes were implanted bilaterally in the VIM in 15(figure 3), and unilaterally on the left in one (014). One of the 15 with bilateral electrodes only had left-sided stimulation (006). One patient also had bilateral electrodes in the Globus Pallidus internus (Gpi) which were OFF at time of testing (008). Mean±sd time since clinical diagnosis was 25±20years. Median time from surgery to testing was 23months (range 1-97months).

Figure 3 here

Steady state AH test

VIM DBS was observed to have modulatory effects causing a relief of AH in thirteen patients, an increase in two and no change in one. Test levels of hypercapnia, ventilation, tidal volume and respiratory frequency were well-matched for ON and OFF conditions (mean±sd $P_{ET}CO_2$ 42.7±4.2 and 42.8±4.4mmHg; mean±sd ventilation 13.7±5.6 and 13.4±4.7L/min; mean±sd VT 0.9±0.5 and 0.9±0.4L; mean±sd fR 16±5.3 and 15.3±3.2 breath per minute. Overall mean SS AH was significantly lower in ON compared to OFF (52.1±27.8 %VAS versus 66.5±20.3 %VAS; figure 4A) with a significant mean reduction of -14.4±15.5%VAS (p=0.002) which exceeds published minimal clinically important difference of 10% for VAS ratings of AH[17, 18]. Individual changes in AH responses with ON condition are displayed in figure 4B.

Figure 4 here

14 participants completed the standard debrief after the initial practice ramp to interrogate the respiratory sensations felt during the practice test. Figure 5 depicts the frequency of descriptors rated according to clusters of AH, Work and Effort (W&E) and 'other' components, showing that patients were able to distinguish AH from the other clusters. Patients commonly confused the mental work associated with the test, with physical work of respiratory muscles; this may account for the high frequency of selecting 'breathing required more work' (figure 5, A).

Figure 5 here

Brain Imaging

Supplementary Figure 4 shows native space thalamic segmentations, confirming appropriate segmentation accuracy. Supplementary Figure 5 demonstrates 3D renderings of each subject's active contacts in native space with individual thalamic segmentations (right column). This was compared with normalised MNI-space electrode reconstructions performed in LeadDBS, with thalamus and VIM estimations from the DISTAL atlas[25], shown for each subject for comparison (left column). This comparison confirms appropriate registration and standard-space normalisation accuracy of the LeadDBS method by an independently Bayesian model-based (FSL/FIRST) approach in subjects' native space.

DISCUSSION

We have systematically studied the effect of motor thalamic DBS on experimentally induced AH in 16 tremor patients. During SS tests, participants gave significantly lower AH ratings when DBS of the VIM was ON (p=0.002). The extent of AH relief (-14.4±15%VAS) exceeded the published minimal clinically important difference [17, 18].

The ascending AH signal via the thalamus

The ascending AH signal is generated by corollary discharge of respiratory drive from the brainstem tempered by vagal afferents from pulmonary stretch receptors reporting prevailing ventilation; Any mismatch modulates the AH signal. This is supported by a variety of evidence, as follows. Gorgon et al (2018) demonstrated that inhaled furosemide sensitised pulmonary stretch receptors relieving hypercapnic induced AH[31]. Fowler et al (1954 showed that rebreathing after breath hold acutely relieved AH in healthy individuals[32]. Flume et al (1996) showed more rapid onset of AH during breath hold and lesser AH relief during rebreathe in lung transplant patients who had fewer pulmonary stretch receptors (PSRs) compared to healthy controls[33].

There remains speculation about the site at which the 'mismatch' comparison occurs. The thalamus has been proposed to gate, and subsequently distribute, the ascending AH signal to cortical sensory areas where AH is consciously perceived. Electrophysiological evidence from studies in cats provides direct evidence for the thalamus representing an intermediary site for the ascending breathlessness signal[15]. In mechanically ventilated paralysed cats, activity of the phrenic nerve, whose firing represents the drive to breathe, was mirrored within thalamic neurons during increasing hypercapnic stimulus once a threshold was reached. It would be interesting to see if this could be confirmed in humans, potentially with the use of iEEG. Human studies also report distinct structural and functional subdivisions of the thalamus being involved in respiratory control receiving respiratory afferents[34].

Role of the thalamus

Functional brain imaging studies report correlations between the activity of thalamic nuclei with both hypercapnic AH and with the sense of breathing effort induced by inspiratory resistive loading[7, 8]. Subregions specifically activated included the dorsomedial, ventrolateral and ventroposterior nuclei. The ventral posterolateral nucleus (VPL), forms part of the sensory thalamus lying posterior to the ventral intermediate nucleus (VIM) and is thought to be a region which can amplify or suppress ascending pain signals[35]. The VPL has also recently been shown to correlate with breathlessness anticipation and its intensity in athletes[36]. Ventroposterior groups have also become DBS targets for neuropathic pain relief, demonstrating their role in sensory processing[37]. The Pulvinar nucleus, the most posterior group, has also been shown to become activated during induced hypercapnia[38]. The VIM itself has not previously been implicated in any brain imaging studies of breathlessness.

Modulation of AH via VIM DBS

The high frequencies (115-155Hz) used to relieve tremor creates a 'reversible lesion' within the field of stimulation preventing aberrant firing patterns within the VIM[39]. DBS disrupts inputs from outputs, determined from its similarities with effects of permanent lesion[40]. We raise the following possible mechanisms of AH relief by VIM DBS (noting that without further imaging analysis, these are highly speculative):

(i) The VIM directly, or indirectly through its connections with nearby sensory nuclei, gates the AH signal to higher areas thus DBS may upregulate this gating control.

(ii) The field of stimulation extends to neighbouring sensory areas that transmit the AH signal. Spread of stimulation to the VPL would be expected to induce paraesthesia in contralateral limbs, as noted with VPL stimulation. The absence of this in the patients reported here undermines this proposed mechanism.

(iii) DBS of the VIM mediates network-wide effects in other areas involved in processing of AH perception, akin to motor cortical stimulation (MCS) for relief of pain, that may act via conferring functional changes in subcortical areas including the thalamus[41] and areas involved in processing of sensory affect such as the anterior cingulate and insula cortex[42]. The motor cortex projects to the thalamus and zona incerta while receiving inputs from thalamic nuclei[43].

(iv) DBS of motor regions proximal to the VIM may have a top down influence on respiratory control as demonstrated in sheep[44]. However, no differences in resting breathing between OFF and ON DBS were observed.

(v) DBS of the VIM has been shown to significantly improve depression[45]. Aggravation of dyspnoea is associated in those with depression and negative affect [46]. Although the causal relationship between the two remains unclear, depressive mood could generate a heightened perception of experimentally induced AH during OFF VIM DBS. Despite pre- and post-operative scores of depression and anxiety not being measured in this study, none of the patients in this cohort had pre-existing depression. In an attempt to interrogate this, albeit in a crude manner, we compared HRV as an indirect indicator of anxiety between ON and OFF DBS in 10 patients and found no differences in root mean square standard deviation of successive differences of RR-interval (Supplementary Figure 2).

Differences in extent of relief

The change in AH with DBS ON ranged from +7.5 to -52.5%VAS. This wide range may be accounted for by differences in the volume of tissue activated (VTA; Supplementary Figure 6) due to appreciable individual variation in position of electrodes and active contacts but could also reflect natural individual variation in the response of the neural tissue to the stimulation.

We posit the following explanations for the variability of electrode positionings and VTA; (i) different electrode trajectories selected during surgery, (ii) differences in active contact selections which were based on largest clinical relief and therefore varied between participants, (iii) that atlas based locations were used for DBS targeting as the VIM is not visible on MRI, which is further confounded by individual variation in brain anatomy and, (iv) differences in amplitude of stimulation, the key determinant of VTA, (see table 1 and figure 3), (v) accuracy by which Lead-DBS can localise electrodes.

Individual differences in strength of connection between the thalamus and regions of interest (ROI's) within the perceptual framework of dyspnoea may also contribute to the heterogeneity in AH relief. The insular cortex is considered to be a principal site for breathlessness perception and is universally and strongly activated in brain imaging studies of breathlessness. Significant connections between insular cortex and thalamus have been demonstrated using high angular resolution diffusion-weighted imaging[47].

Reports from functional resting state activity also show a connection between the thalamus and insula. Wiech et al, (2014) reported the most significant region connected with the anterior, mid, and posterior insula was the thalamus, with the anterior insula and thalamus representing the strongest connectivity of all subregions[48].

Therefore, the strength of structural and functional connectivity between the thalamus and insular cortex may differ between individuals thereby explaining variation in AH relief with DBS.

One point to consider is the influence of tremor on respiratory muscle activity, and whether tremor relief during ON DBS is correlated with relief in AH. DBS could influence respiratory muscle activity, potentially impacting the overall sensation of dyspnoea. Respiratory flutter at the same frequency of tremor (4-8Hz) has been observed on the flow volume loop in patients with PD which was correlated with dyskinesia and tremor[49]. The question as to whether this is tremor of the respiratory muscles themselves, or other muscles in the chest or neck remains an open one. However, if it is respiratory muscles that tremor, this is more likely to cause changes in sense of breathing work and effort rather than air hunger. Evidence for this includes complete neuromuscular block experiments showing that respiratory muscle feedback is not involved in air hunger perception[50, 51]. Furthermore, vibration of respiratory muscles has been shown to have no effect on AH[52]. Nonetheless, it would be interesting to assess the sense of breathing work and effort with diaphragmatic EMG alongside experimentally induced AH in a cohort of this type. In our cohort, we found no correlation between tremor improvement and extent of AH relief (Supplementary Figure 3, r^2=0.04, p=>0.05 spearman's correlation).

Limitations

(i) The frequencies and amplitudes of the DBS in this patient group are in accordance with individual optimal tremor relief. We do not know if these stimulus parameters are also optimal for breathlessness relief.

(ii) As steady state tests were conducted with bilateral electrodes either OFF or ON, we cannot make assumptions about laterality of the DBS effects on AH relief.

(iii) The time since surgery to test-date varied considerably among participants (range 1-97 months). However, there seemed to be no correlation between time since DBS surgery and the extent of AH modulation from OFF to ON DBS (Supplementary material; Figure 1).

(iv) To see if there was any order effect which could explain the AH relief with DBS ON, we compared the extent of relief between those who completed the AH with DBS ON first versus those who completed the AH tests with DBS OFF first (Mean AH relief ON first=15.1±25.2, Mean AH relief OFF first=14.2±12.5, p=0.95 unpaired t-test). Thus, we found no evidence of an order effect in our dataset.

CONCLUSIONS

We have shown that DBS of the motor thalamus is associated with a significant relief of experimentally induced hypercapnic air hunger in patients with tremor. The possible mechanism of relief by stimulation of the VIM is not yet defined. We propose that DBS creates a 'virtual lesion' that somewhat negates the ascending air hunger signal ascending via the thalamus dampening its distribution to perceptual areas of dyspnoea.

The extent of relief suggests that DBS or non-invasive stimulation of the VIM, or other thalamic sensory nuclei, may prove to be a viable therapy for intractable dyspnoea in severe cases where a patient's breathlessness has proven to be refractory to current treatment options. This form of treatment based on DBS of the thalamic sensory nuclei has already been explored for chronic pain[37]. This study advances our understanding of the cerebral mechanisms of breathlessness, in particular its route prior to conscious awareness while the potential clinical applications warrant further investigation.

Funding

Chapman TP was funded by the Nigel Groome Studentship provided by Oxford Brookes University. Green AL is funded by the NIHR Biomedical Research Centre.

Conflict of Interest

Authors declare that they have no major conflict of interests.

Table 1: Demographics, clinical characteristics, and deep brain stimulation parameters.

Abbreviations: VIM; Ventral Intermediate Nucleus, Bilat; Bilateral, ET; Essential Tremor, DT; Dystonic Tremor, PD; Parkinson's Disease.

ID	Age	Sex	Ht (cm)	Wt (lbs)	DBS	Tremor	Disease Duration (months)	Medications	Time since DBS (months)	CO-morbidities	Amp (mA/V) L	R	Pulse width (us) L	R
1	69	M	170	212	Bilat Vim	DT	14	Candesartan, Dipyridamole, Duloxetine, Simvastatin	1	Previous Stroke	2.9		3.5	
2	75	M	171	187	Bilat Vim	ET	15	None	1	Irregular heartbeat	2		2	
3	75	M	164	165	Bilat Vim	ET	12	None	35	OCD	3	3	80	70
4	67	M	177	170	Bilat Vim	ET	10	None	36	None	4.15	1.2	90	90
5	40	F	169	165	Bilat Vim	ET	51	Propanolol 40mg	6	None	1.4	1.5	80	80
6	63	M	182	143	Bilat Vim L side ON	ET	57	Clindamycin	12	None	3.5	/	180	60
7	53	F	173	154	Bilat Vim	DT	2	None	3	None	1.5	2.2	70	70
8	73	F	163	185	Bilat Vim	ET+DT features	40	Atenolol, Candesartan, Pravastatin, Fusidic acid	25	High blood pressure	2.2	2	110	/

9	72	M	182	220	Bilat Vim	ET	7	Sodium Valproate, Felodipine, Bisoprolol, Aspirin, Atorvastatin	20	Acute STEMI, Smoker, Osteoarthritis, BCC, Epilepsy	3.4	2.15	90	90
10	74	M	180	177	Bilat Vim	ET	70	Apixaban, Digoxin, Clonazepam, salbutamol, salmeterol inhaler, Calcichew,	4	Subependymal lesion, Asthma	2.3	2.2	120	100
11	75	M	180	169	Bilat Vim	ET	12	None	50	None	2.3	2.3	120	80
12	75	M	162	162	Bilat Vim	ET	14	None	97	None	2.1	2.1	80	80
13	69	M	176	209	Bilat Vim	ET	11	Candesartan, Amlodipine, Lansoprazole, Tolterodine	37	Hypertension, cataract L eye, acute ulcerative colitis, stomach ulcer, urinary urgency	1.5	0.7	70	70
14	71	M	190	227	L Vim	PD	27	Sinemet, Pramipexole, Opicapone	55	None	2.5	/	60	80

15	59	M	178	182	Bilat Vim	PD	18	Stalevo, Sinemet, quetiapine	91	None	5.3	3.5	70	70
16	59	M	174	209	Bilat Vim	ET	33	None	12	Smoker, overactive bladder	0.75	3	70	/

Supplementary materials

Table 2: Typical verbatim comments after experiencing hypercapnic induced air hunger in ramp and SS tests. All comments were volunteered by participants during the course of the standard debrief questionnaire.

Participant	Comment
P005	[Felt a] shortness of breath.
P006	No oxygen there.
P008	Can't get enough air. Shortness of breath. A starvation.
P009	Felt like I wasn't taking in any air. Felt like the tubing was blocked and there was nothing useful.
P011	[Felt like] being starved of air
P015	The test (SS) felt far easier when my DBS was ON

Supplementary Figure 1

Figure Legends

Figure 1 Experimental setup and protocol. Panel A, *experimental setup: Participants breathed via a mouthpiece from a 3 Litre anaesthetic bag into which the flow of fresh gas was set to the participants' baseline minute ventilation (VE). A Metronome was used to set breathing frequency (fR) to the participants' spontaneous rate at baseline.* ***Panel B****: Protocol: During the first RAMP test (RAMP 1), one-minute increments in inspired CO_2 were implemented using a gas blender which mixed medical gases from compressed gas cylinders, while participants rated any breathing discomfort on a 100mm visual analogue scale. The standard debrief afterward ensured that participants recognised air hunger as a dominant component of their respiratory discomfort and that they had used the VAS correctly. During steady state tests a constant level of inspired CO2 was imposed targeting 50% full scale of the VAS which was determined from the initial practice ramp test. Abbreviations: VE=Minute ventilation, fR= Breathing frequency, VT=Tidal Volume, PCO_2=End-tidal CO_2, PAW=Airway pressure, RD=Respiratory discomfort, DBS= Deep brain stimulation.*

Figure 2: Physiological recordings during ramp and steady state hypercapnic air hunger tests. Panel A: *Raw physiological traces for air hunger (AH), PCO2, airway pressure (PAW) and tidal volume (VT) during the practice hypercapnic ramp with constrained ventilation in both OFF and ON DBS conditions.* ***Panel B****; Raw physiological traces during the hypercapnic steady state air hunger tests. Variables which lie within the last minute of the test (Green Box) were processed and compared between ON and OFF DBS conditions. Abbreviations: AH=Air hunger, PCO_2=End-tidal PCO_2, PAW=Airway pressure, VT=Tidal volume.*

Figure 3 DBS electrodes and their active contacts in relation to the VIM for 15 participants visualised in standard MNI space using Lead-DBS V3 software. Panel A; *Shows the electrode positionings (solid grey electrodes) within MNI space(25) with the VIM visualised using DISTAL-medium atlas(29).* ***Panel B;*** *Transparent electrodes and their active contacts.* ***Panel C;*** *Point-cloud visualisation of active contacts, with their colour correlated to extent of AH relief from OFF to ON DBS. Colour of dots represent extent of relief with blue (most relief) to red (least relief/heightening).*

Figure 4 Effect of deep brain stimulation of the VIM on hypercapnic air hunger. Panel A*: Box and whisker plot showing the median and mean (horizontal solid, and dashed line, respectively), Interquartile range (shaded boxes), and upper/lower extremes (whiskers) for ratings of air hunger (AH) on a 100mm visual analogue scale (VAS) during experimentally induced steady state hypercapnic air hunger with constrained ventilation with deep brain stimulation (DBS) electrodes in the VIM with DBS switched off (OFF) and switched on (ON) in 16 tremor patients.* ***Panel B****: The change in %VAS air hunger responses when DBS of the VIM is switched ON. The dotted line represents the minimal clinically important difference of 10%VAS for VAS ratings of AH (17;18). Abbreviations: DBS=Deep brain stimulation.*

Figure 5 Respiratory descriptors associated with the initial practice ramp. *The frequency of choosing air hunger (AH), work and effort (W&E) and the 'other' cluster of descriptors as one of the top three sensations experienced at the peak of the initial practice hypercapnic ramp test. Participants were instructed to rate any breathing discomfort during this test.* ***Panel A***

represents the frequency of each descriptor while ***panel B*** *represents the sum of each cluster of descriptors according to their category Abbreviations: AH=Air hunger, W&E= Sense of breathing work and effort.*

Supplementary figure 1: Relationship between time from DBS surgery to testing. *Changes in AH responses during experimentally induced hypercapnic steady state tests were plotted against time from DBS surgery to testing date (months). Abbreviation: AH= Air hunger, DBS=Deep brain stimulation.*

Supplementary figure 2: Effect of DBS on Heart rate variability. *Left panel; The root mean square of successive differences (RMSSD) in R-R interval during ON and OFF VIM DBS in 10 patients are compared as box and whisker plots. Right panel; Individual relief of AH with ON VIM DBS plotted as a function of individual change in HRV. Abbreviations; RMSSD= Root mean square of successive differences.*

Supplementary figure 3: Improvement in tremor versus AH relief during VIM DBS. *Individual changes in AH with VIM DBS plotted as a function of percent change in global tremor. Abbreviations; AH= Air hunger, VIM=Ventral intermediate nucleus, DBS=Deep brain stimulation.*

Supplementary figure 4: Native space individual thalamic segmentations. *Visual representation of individual thalamic segmentations (red outline) presented in the sagittal, coronal and axial planes.*

Supplementary figure 5: Verification of leadDBS electrode positioning in leadDBS versus in native space. 3D renderings of each subject's active contacts (red; anode, blue; cathode) in native space with individual thalamic (yellow/orange) segmentations (right column). This was compared with normalised MNI-space electrode reconstructions performed in LeadDBS (left column), with thalamus and VIM estimations from the DISTAL atlas (24). This comparison confirms appropriate registration and standard-space normalisation accuracy of the LeadDBS method by an independently Bayesian model-based (FSL/FIRST) approach in subjects' native space. Abbreviations; VIM=Ventral i*ntermediate* n*ucleus,* MNI=Montreal Neurological Institute.

Supplementary Figure 6: Field of stimulations for DBS electrodes. 3D renderings of VTAs for each subject in MNI space using LeadDBS. The VTA colour is correlated with the extent of AH modulation (%VAS) during VIM DBS. Abbreviations: VIM=Ventral intermediate nucleus, VTA= Volume of tissue activated, MNI=Montreal Neurological Institute, AH=Air hunger.

REFERENCES

1. Parshall MB, Schwartzstein RM, Adams L, Banzett RB, Manning HL, Bourbeau J, Calverley PM, Gift AG, Harver A, Lareau SC, Mahler DA, Meek PM, O'Donnell DE. An official American Thoracic Society statement: update on the mechanisms, assessment, and management of dyspnea. *Am J Respir Crit Care Med* 2012: 185(4): 435-452.
2. Ho SF, O'Mahony MS, Steward JA, Breay P, Buchalter M, Burr ML. Dyspnoea and quality of life in older people at home. *Age Ageing* 2001: 30(2): 155-159.
3. Lansing RW, Im BSH, Thwing JI, Legedza ATR, Banzett RB. The perception of respiratory work and effort can be independent of the perception of air hunger. *American Journal of Respiratory and Critical Care Medicine* 2000: 162(5): 1690-1696.
4. O'Donnell DE, Banzett RB, Carrieri-Kohlman V, Casaburi R, Davenport PW, Gandevia SC, Gelb AF, Mahler DA, Webb KA. Pathophysiology of dyspnea in chronic obstructive pulmonary disease: a roundtable. *Proc Am Thorac Soc* 2007: 4(2): 145-168.
5. Moosavi SH, Topulos GP, Hafer A, Lansing RW, Adams L, Brown R, Banzett RB. Acute partial paralysis alters perceptions of air hunger, work and effort at constant P(CO(2)) and V(E). *Respir Physiol* 2000: 122(1): 45-60.
6. O'Donnell CR, Schwartzstein RM, Lansing RW, Guilfoyle T, Elkin D, Banzett RB. Dyspnea affective response: comparing COPD patients with healthy volunteers and laboratory model with activities of daily living. *BMC Pulm Med* 2013: 13: 27.
7. Evans KC, Banzett RB, Adams L, McKay L, Frackowiak RS, Corfield DR. BOLD fMRI identifies limbic, paralimbic, and cerebellar activation during air hunger. *J Neurophysiol* 2002: 88(3): 1500-1511.
8. von Leupoldt A, Sommer T, Kegat S, Baumann HJ, Klose H, Dahme B, Büchel C. Dyspnea and pain share emotion-related brain network. *Neuroimage* 2009: 48(1): 200-206.
9. Banzett RB, Mulnier HE, Murphy K, Rosen SD, Wise RJ, Adams L. Breathlessness in humans activates insular cortex. *Neuroreport* 2000: 11(10): 2117-2120.
10. von Leupoldt A, Sommer T, Kegat S, Baumann HJ, Klose H, Dahme B, Büchel C. The unpleasantness of perceived dyspnea is processed in the anterior insula and amygdala. *Am J Respir Crit Care Med* 2008: 177(9): 1026-1032.
11. Peiffer C, Poline JB, Thivard L, Aubier M, Samson Y. Neural substrates for the perception of acutely induced dyspnea. *Am J Respir Crit Care Med* 2001: 163(4): 951-957.
12. Hayen A, Wanigasekera V, Faull OK, Campbell SF, Garry PS, Raby SJM, Robertson J, Webster R, Wise RG, Herigstad M, Pattinson KTS. Opioid suppression of conditioned anticipatory brain responses to breathlessness. *Neuroimage* 2017: 150: 383-394.
13. Sankar T, Tierney TS, Hamani C. Novel applications of deep brain stimulation. *Surg Neurol Int* 2012: 3(Suppl 1): S26-33.
14. Green AL, Debrah E, Roy HA, Rebelo P, Moosavi SH. Letter to the editor: Thalamic deep brain stimulation may relieve breathlessness in COPD. *Brain Stimul* 2019: 12(3): 827-828.
15. Chen Z, Eldridge FL, Wagner PG. Respiratory-associated thalamic activity is related to level of respiratory drive. *Respir Physiol* 1992: 90(1): 99-113.
16. Banzett RB, Lansing RW, Evans KC, Shea SA. Stimulus-response characteristics of CO2-induced air hunger in normal subjects. *Respir Physiol* 1996: 103(1): 19-31.
17. Ries AL. Minimally clinically important difference for the UCSD Shortness of Breath Questionnaire, Borg Scale, and Visual Analog Scale. *Copd* 2005: 2(1): 105-110.

18. Ekström M, Johnson MJ, Huang C, Currow DC. Minimal clinically important differences in average, best, worst and current intensity and unpleasantness of chronic breathlessness. *Eur Respir J* 2020: 56(2).
19. Lansing R, R B. Lansing R, R B. Psychophysical methods in the study of respiratory sensation. In: AdamsL, Guz A, editors: Respiratory sensation, lung biology in health and disease. New York: Marcel Dekker; 1996. pp.69-100.
20. Horn A, Kühn AA. Lead-DBS: a toolbox for deep brain stimulation electrode localizations and visualizations. *Neuroimage* 2015: 107: 127-135.
21. Avants BB, Epstein CL, Grossman M, Gee JC. Symmetric diffeomorphic image registration with cross-correlation: evaluating automated labeling of elderly and neurodegenerative brain. *Med Image Anal* 2008: 12(1): 26-41.
22. Fonov V, Evans AC, Botteron K, Almli CR, McKinstry RC, Collins DL. Unbiased average age-appropriate atlases for pediatric studies. *Neuroimage* 2011: 54(1): 313-327.
23. Husch A, M VP, Gemmar P, Goncalves J, Hertel F. PaCER - A fully automated method for electrode trajectory and contact reconstruction in deep brain stimulation. *Neuroimage Clin* 2018: 17: 80-89.
24. Dembek TA, Asendorf AL, Wirths J, Barbe MT, Visser-Vandewalle V, Treuer H. Temporal Stability of Lead Orientation in Directional Deep Brain Stimulation. *Stereotact Funct Neurosurg* 2021: 99(2): 167-170.
25. Ewert S, Plettig P, Li N, Chakravarty MM, Collins DL, Herrington TM, Kühn AA, Horn A. Toward defining deep brain stimulation targets in MNI space: A subcortical atlas based on multimodal MRI, histology and structural connectivity. *Neuroimage* 2018: 170: 271-282.
26. Treu S, Strange B, Oxenford S, Neumann WJ, Kühn A, Li N, Horn A. Deep brain stimulation: Imaging on a group level. *Neuroimage* 2020: 219: 117018.
27. Jenkinson M, Smith S. A global optimisation method for robust affine registration of brain images. *Med Image Anal* 2001: 5(2): 143-156.
28. Jenkinson M, Bannister P, Brady M, Smith S. Improved optimization for the robust and accurate linear registration and motion correction of brain images. *Neuroimage* 2002: 17(2): 825-841.
29. Smith SM, Jenkinson M, Woolrich MW, Beckmann CF, Behrens TE, Johansen-Berg H, Bannister PR, De Luca M, Drobnjak I, Flitney DE, Niazy RK, Saunders J, Vickers J, Zhang Y, De Stefano N, Brady JM, Matthews PM. Advances in functional and structural MR image analysis and implementation as FSL. *Neuroimage* 2004: 23 Suppl 1: S208-219.
30. Patenaude B, Smith SM, Kennedy DN, Jenkinson M. A Bayesian model of shape and appearance for subcortical brain segmentation. *Neuroimage* 2011: 56(3): 907-922.
31. Grogono JC, Butler C, Izadi H, Moosavi SH. Inhaled furosemide for relief of air hunger versus sense of breathing effort: a randomized controlled trial. *Respir Res* 2018: 19(1): 181.
32. Fowler WS. Breaking point of breath-holding. *J Appl Physiol* 1954: 6(9): 539-545.
33. Flume PA, Eldridge FL, Edwards LJ, Mattison LE. Relief of the 'air hunger' of breathholding. A role for pulmonary stretch receptors. *Respir Physiol* 1996: 103(3): 221-232.
34. Pattinson KT, Mitsis GD, Harvey AK, Jbabdi S, Dirckx S, Mayhew SD, Rogers R, Tracey I, Wise RG. Determination of the human brainstem respiratory control network and its cortical connections in vivo using functional and structural imaging. *Neuroimage* 2009: 44(2): 295-305.
35. Ziegler K, Folkard R, Gonzalez AJ, Burghardt J, Antharvedi-Goda S, Martin-Cortecero J, Isaías-Camacho E, Kaushalya S, Tan LL, Kuner T, Acuna C, Kuner R, Mease RA, Groh A. Primary somatosensory cortex bidirectionally modulates sensory gain and nociceptive behavior in a layer-specific manner. *Nat Commun* 2023: 14(1): 2999.
36. Faull OK, Cox PJ, Pattinson KTS. Cortical processing of breathing perceptions in the athletic brain. *Neuroimage* 2018: 179: 92-101.
37. Boccard SG, Pereira EA, Moir L, Aziz TZ, Green AL. Long-term outcomes of deep brain stimulation for neuropathic pain. *Neurosurgery* 2013: 72(2): 221-230; discussion 231.

38. Brannan S, Liotti M, Egan G, Shade R, Madden L, Robillard R, Abplanalp B, Stofer K, Denton D, Fox PT. Neuroimaging of cerebral activations and deactivations associated with hypercapnia and hunger for air. *Proc Natl Acad Sci U S A* 2001: 98(4): 2029-2034.
39. Benazzouz A, Hallett M. Mechanism of action of deep brain stimulation. *Neurology* 2000: 55(12 Suppl 6): S13-16.
40. Dallapiazza RF, Lee DJ, De Vloo P, Fomenko A, Hamani C, Hodaie M, Kalia SK, Fasano A, Lozano AM. Outcomes from stereotactic surgery for essential tremor. *J Neurol Neurosurg Psychiatry* 2019: 90(4): 474-482.
41. Henssen D, Giesen E, van der Heiden M, Kerperien M, Lange S, van Cappellen van Walsum AM, Kurt E, van Dongen R, Schutter D, Vissers K. A systematic review of the proposed mechanisms underpinning pain relief by primary motor cortex stimulation in animals. *Neurosci Lett* 2020: 719: 134489.
42. García-Larrea L, Peyron R, Mertens P, Gregoire MC, Lavenne F, Le Bars D, Convers P, Mauguière F, Sindou M, Laurent B. Electrical stimulation of motor cortex for pain control: a combined PET-scan and electrophysiological study. *Pain* 1999: 83(2): 259-273.
43. Sherman SM. Thalamus plays a central role in ongoing cortical functioning. *Nat Neurosci* 2016: 19(4): 533-541.
44. Koos BJ, Kawasaki Y, Hari A, Bohorquez F, Jan C, Roostaeian J, Wilson CL, Kruger L. Electrical stimulation of the posteromedial thalamus modulates breathing in unanesthetized fetal sheep. *J Appl Physiol (1985)* 2004: 96(1): 115-123.
45. Gupta R, Paulo D, Sun L, Ye F, Dhima K, Bick SK. Depression Scores following Ventral Intermediate Nucleus Deep Brain Stimulation for Essential Tremor: A Meta-Analysis. Stereotact Funct Neurosurg. © 2023 S. Karger AG, Basel., Switzerland, 2023; pp. 170-178.
46. Rahi MS, Thilagar B, Balaji S, Prabhakaran SY, Mudgal M, Rajoo S, Yella PR, Satija P, Zagorulko A, Gunasekaran K. The Impact of Anxiety and Depression in Chronic Obstructive Pulmonary Disease. *Adv Respir Med* 2023: 91(2): 123-134.
47. Nomi JS, Schettini E, Broce I, Dick AS, Uddin LQ. Structural Connections of Functionally Defined Human Insular Subdivisions. *Cereb Cortex* 2018: 28(10): 3445-3456.
48. Wiech K, Jbabdi S, Lin CS, Andersson J, Tracey I. Differential structural and resting state connectivity between insular subdivisions and other pain-related brain regions. *Pain* 2014: 155(10): 2047-2055.
49. Hovestadt A, Bogaard JM, Meerwaldt JD, van der Meché FG, Stigt J. Pulmonary function in Parkinson's disease. *J Neurol Neurosurg Psychiatry* 1989: 52(3): 329-333.
50. Banzett RB, Lansing RW, Brown R, Topulos GP, Yager D, Steele SM, Londoño B, Loring SH, Reid MB, Adams L, et al. 'Air hunger' from increased PCO2 persists after complete neuromuscular block in humans. *Respir Physiol* 1990: 81(1): 1-17.
51. Gandevia SC, Killian K, McKenzie DK, Crawford M, Allen GM, Gorman RB, Hales JP. Respiratory sensations, cardiovascular control, kinaesthesia and transcranial stimulation during paralysis in humans. *J Physiol* 1993: 470: 85-107.
52. Bloch-Salisbury E, Binks AP, Banzett RB, Schwartzstein RM. Mechanical chest-wall vibration does not relieve air hunger. *Respir Physiol Neurobiol* 2003: 134(3): 177-190.

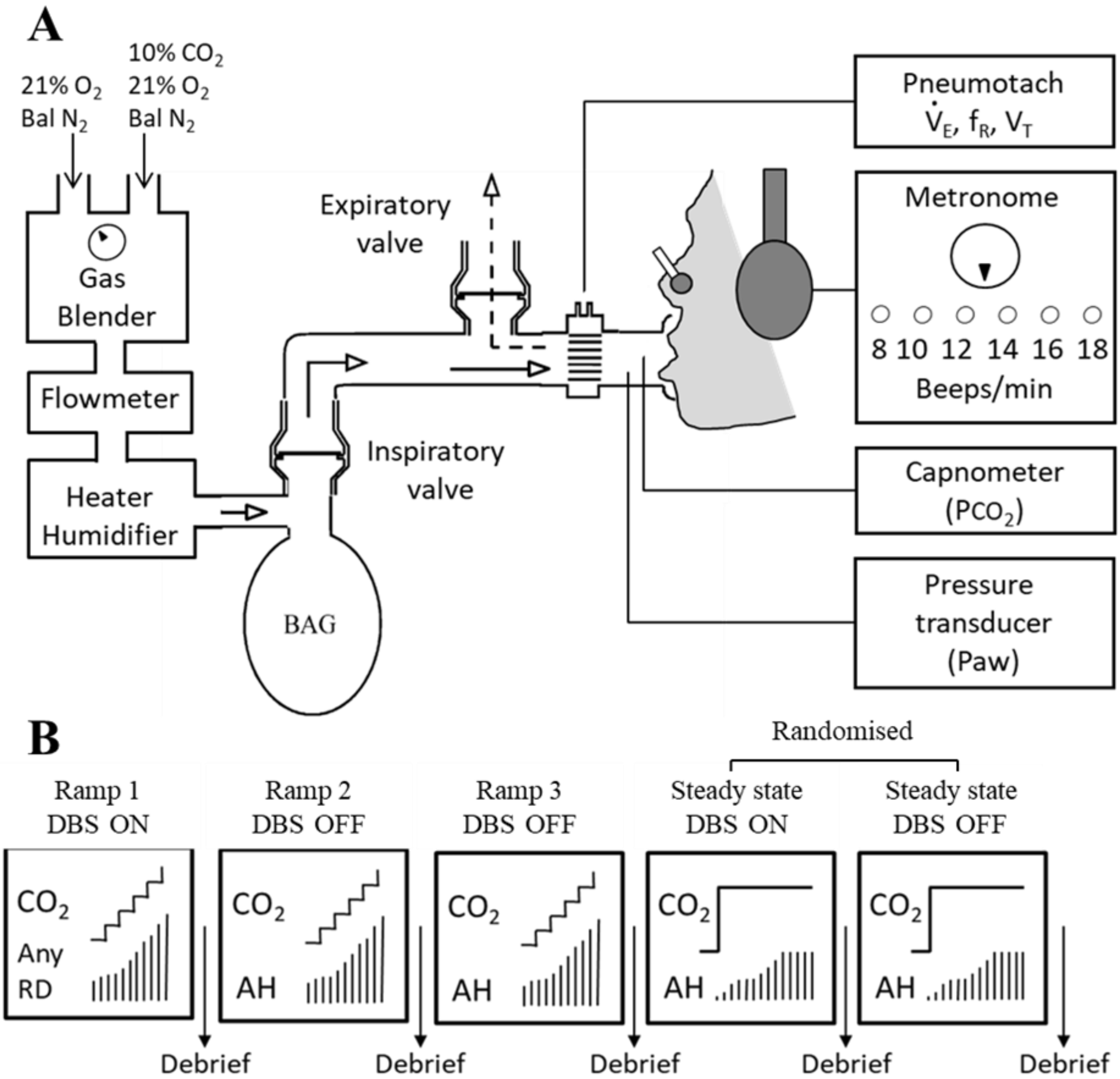
A
10% CO2
21% O2
Bal N2
21% O2
Bal N2
Gas
Blender
Flowmeter
Heater
Humidifier
BAG
Expiratory
valve
Inspiratory
valve
Pneumotach
V̇E, fR, VT
Metronome
8 10 12 14 16 18
Beeps/min
Capnometer
(PCO2)
Pressure
transducer
(Paw)
B
Randomised
Ramp 1
DBS ON
Ramp 2
DBS OFF
Ramp 3
DBS OFF
Steady state
DBS ON
Steady state
DBS OFF
CO2
Any
RD
AH
Debrief

Figure 1

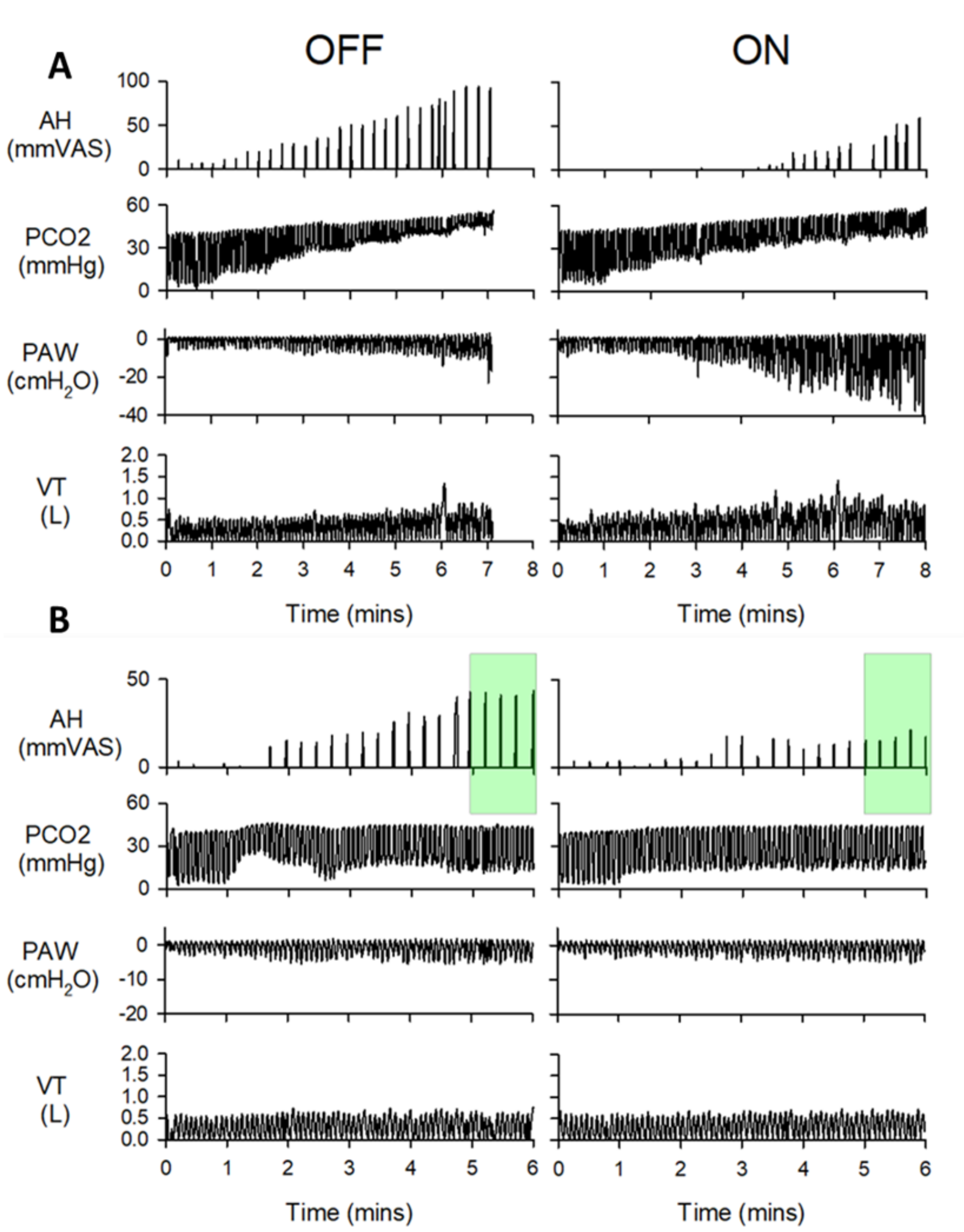
A
OFF
ON
AH
(mmVAS)
100
50
0
PCO2
(mmHg)
60
30
0
PAW
(cmH2O)
0
-20
-40
VT
(L)
2.0
1.5
1.0
0.5
0.0
0 1 2 3 4 5 6 7 8
Time (mins)
B
AH
(mmVAS)
50
0
PCO2
(mmHg)
60
30
0
PAW
(cmH2O)
0
-10
-20
VT
(L)
2.0
1.5
1.0
0.5
0.0
0 1 2 3 4 5 6
Time (mins)

Figure 2

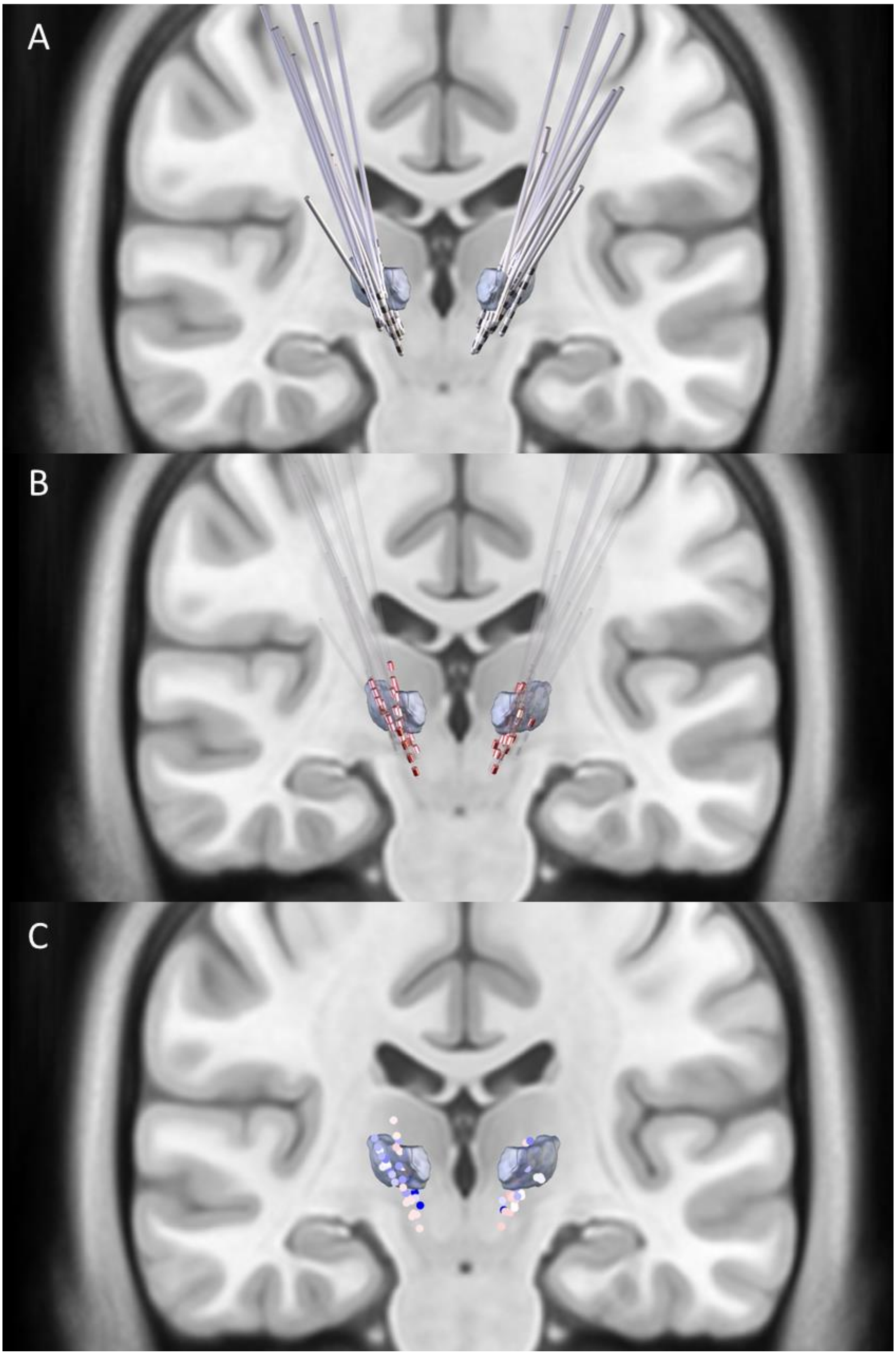

Figure 3

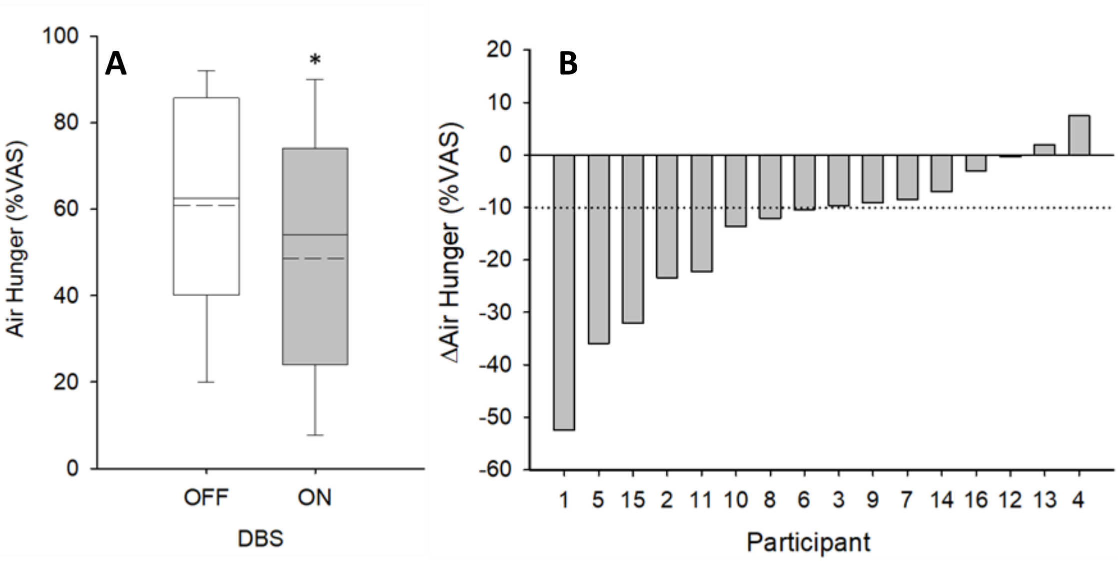
A
B
Air Hunger (%VAS)
OFF
ON
DBS
*
100
80
60
40
20
0
ΔAir Hunger (%VAS)
20
10
0
-10
-20
-30
-40
-50
-60
1 5 15 2 11 10 8 6 3 9 7 14 16 12 13 4
Participant

Figure 4

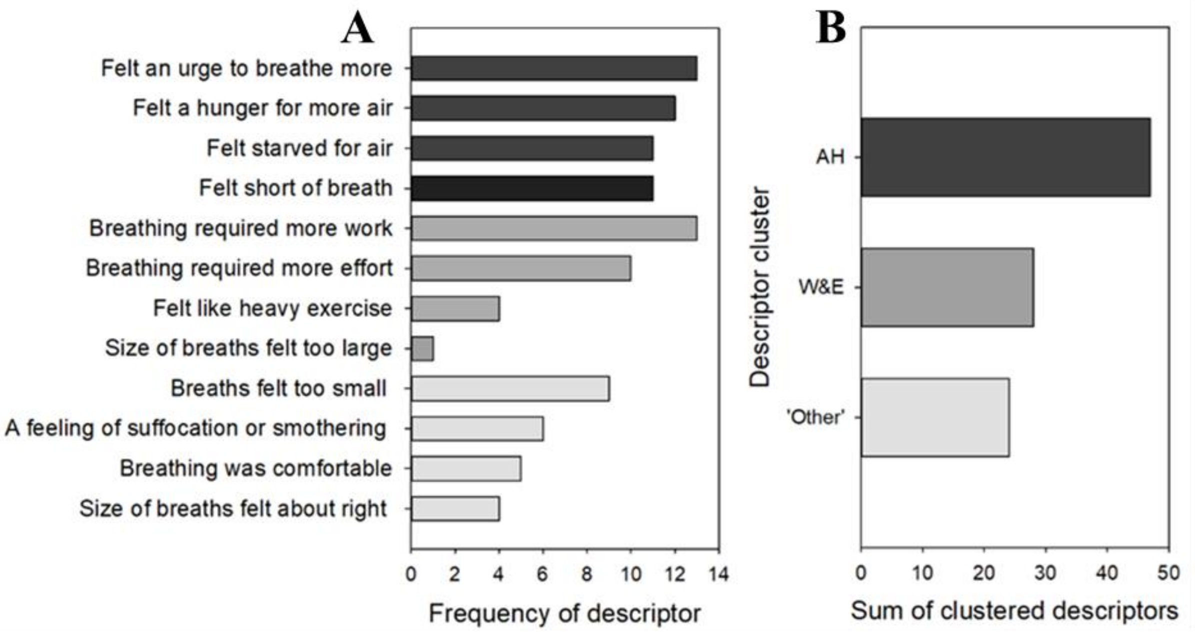
A
Felt an urge to breathe more
Felt a hunger for more air
Felt starved for air
Felt short of breath
Breathing required more work
Breathing required more effort
Felt like heavy exercise
Size of breaths felt too large
Breaths felt too small
A feeling of suffocation or smothering
Breathing was comfortable
Size of breaths felt about right
0 2 4 6 8 10 12 14
Frequency of descriptor
B
Descriptor cluster
AH
W&E
'Other'
0 10 20 30 40 50
Sum of clustered descriptors

Figure 5

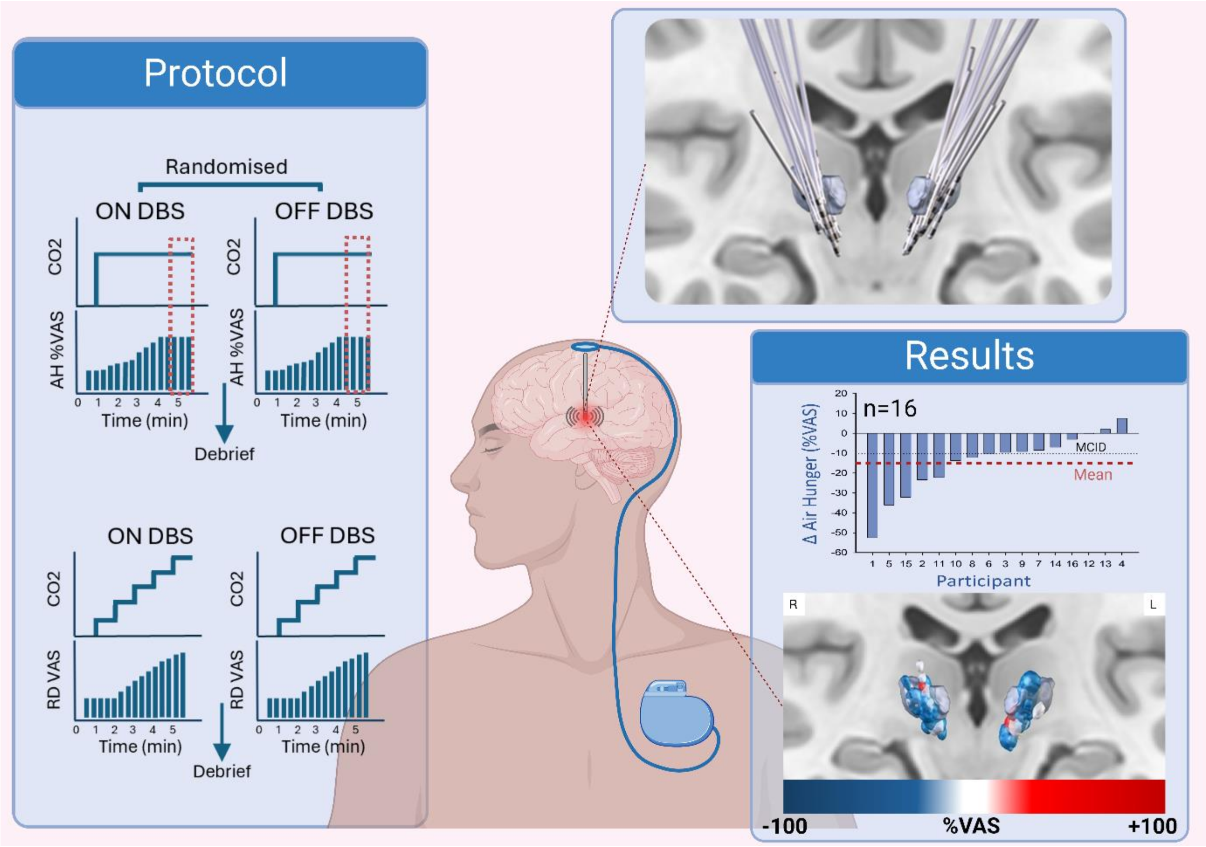
Protocol
Randomised
ON DBS
OFF DBS
CO2
AH %VAS
Time (min)
Debrief
ON DBS
OFF DBS
CO2
RD VAS
Time (min)
Debrief
Results
n=16
Δ Air Hunger (%VAS)
MCID
Mean
Participant
R
L
-100
%VAS
+100

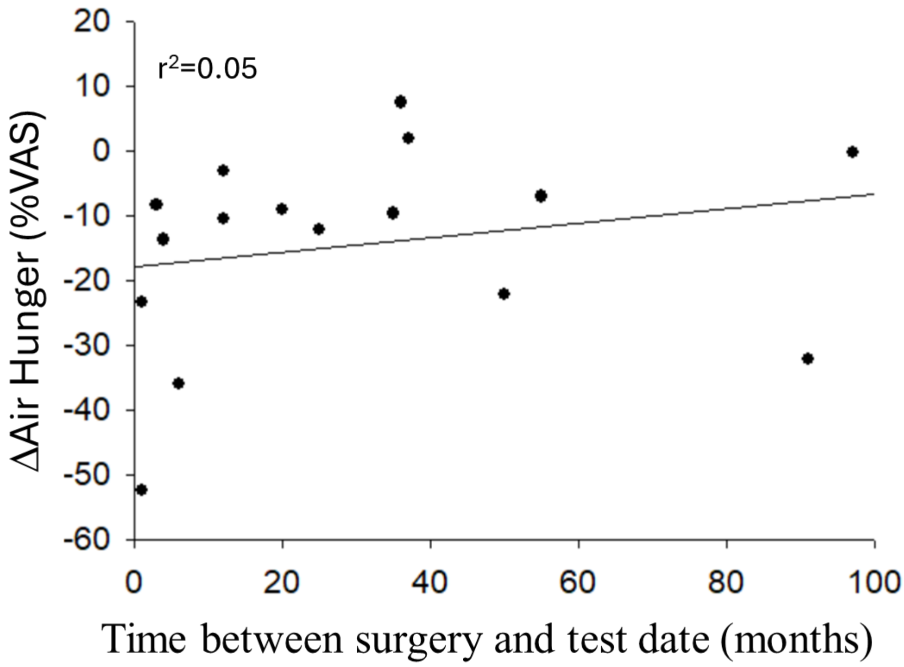
r²=0.05
20
10
0
-10
-20
-30
-40
-50
-60
ΔAir Hunger (%VAS)
0
20
40
60
80
100
Time between surgery and test date (months)

Figure S1

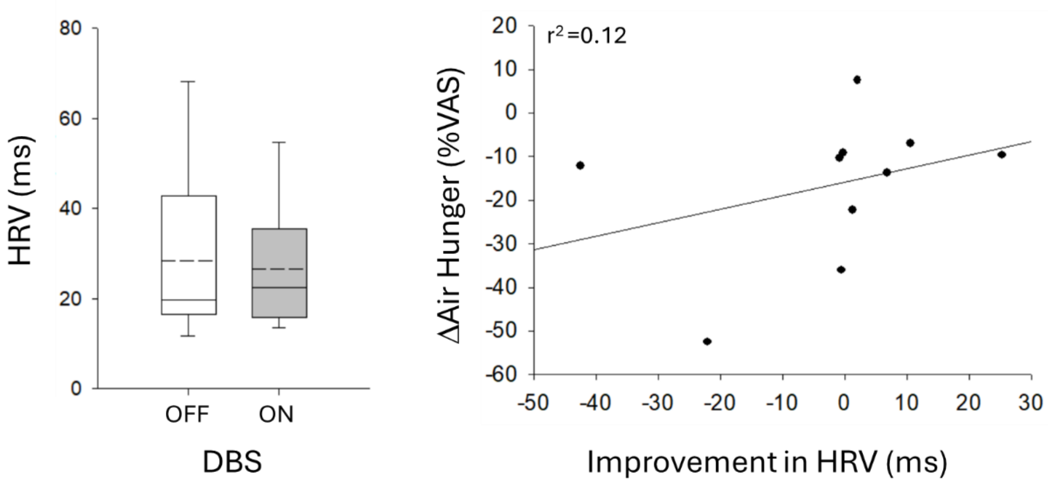
80
60
40
20
0
HRV (ms)
OFF
ON
DBS
20
10
0
-10
-20
-30
-40
-50
-60
r^2=0.12
ΔAir Hunger (%VAS)
-50
-40
-30
-20
-10
0
10
20
30
Improvement in HRV (ms)

Figure S2

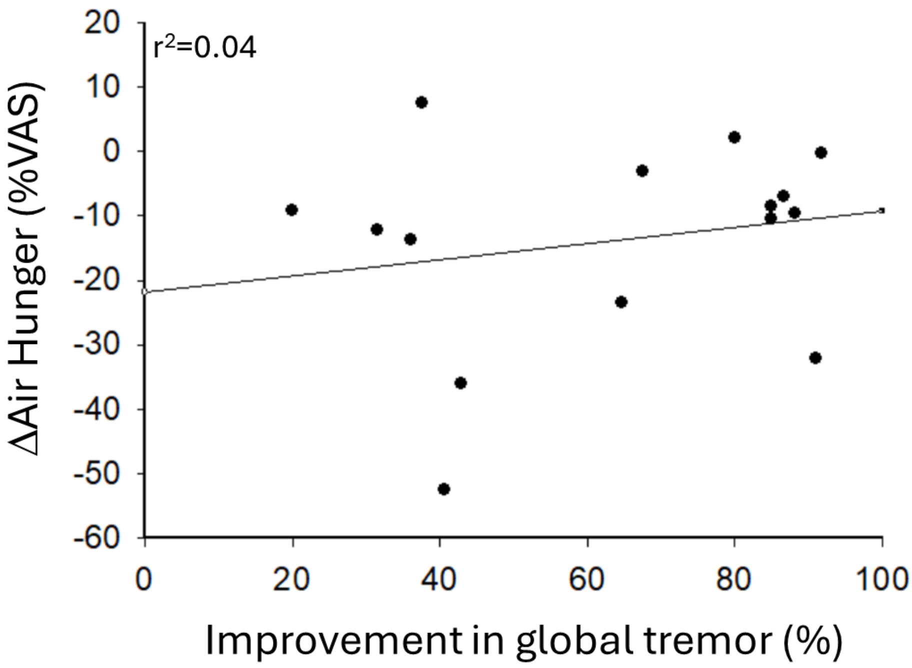
r²=0.04
ΔAir Hunger (%VAS)
20
10
0
-10
-20
-30
-40
-50
-60
0
20
40
60
80
100
Improvement in global tremor (%)

Figure S3

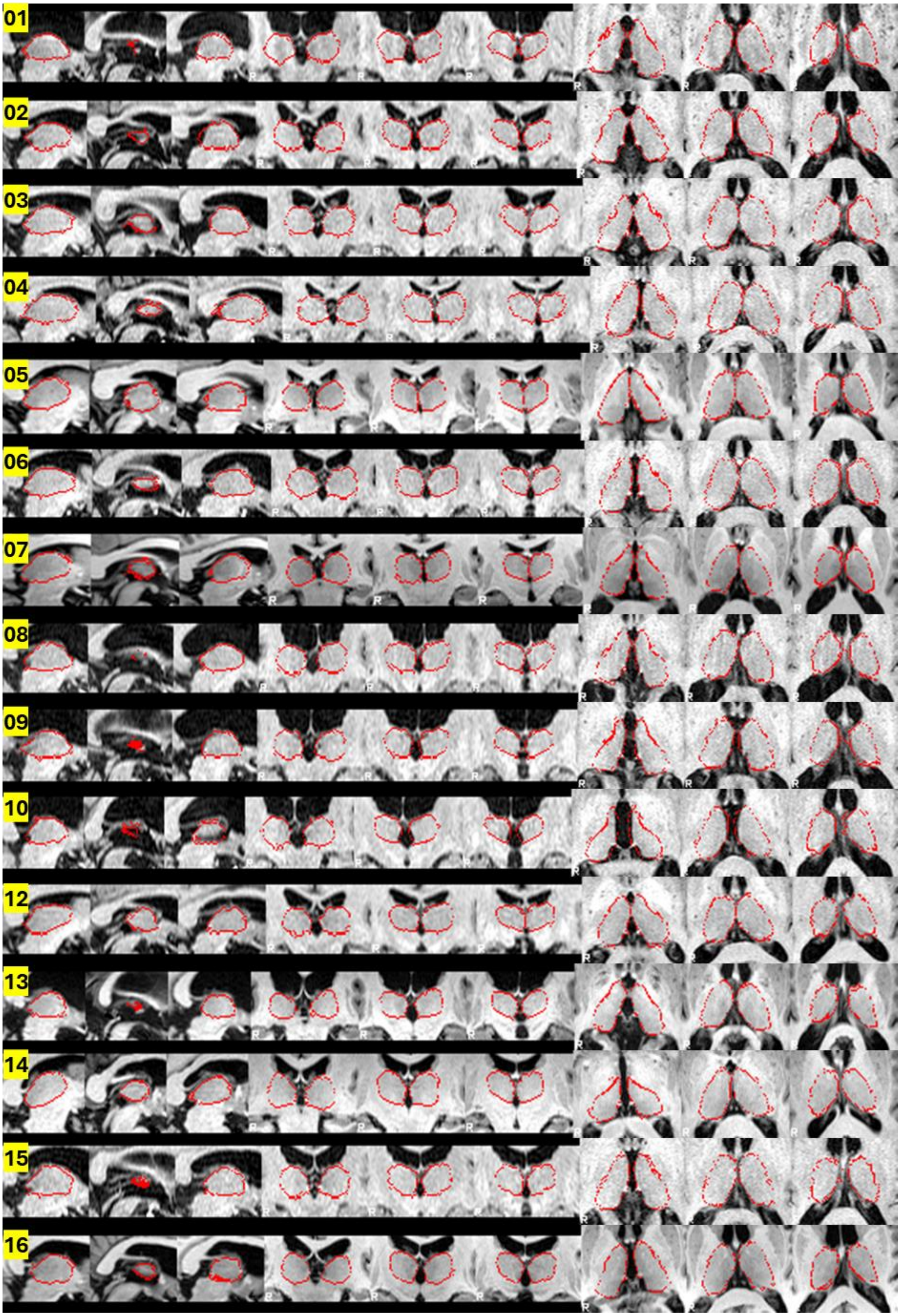

Figure S4

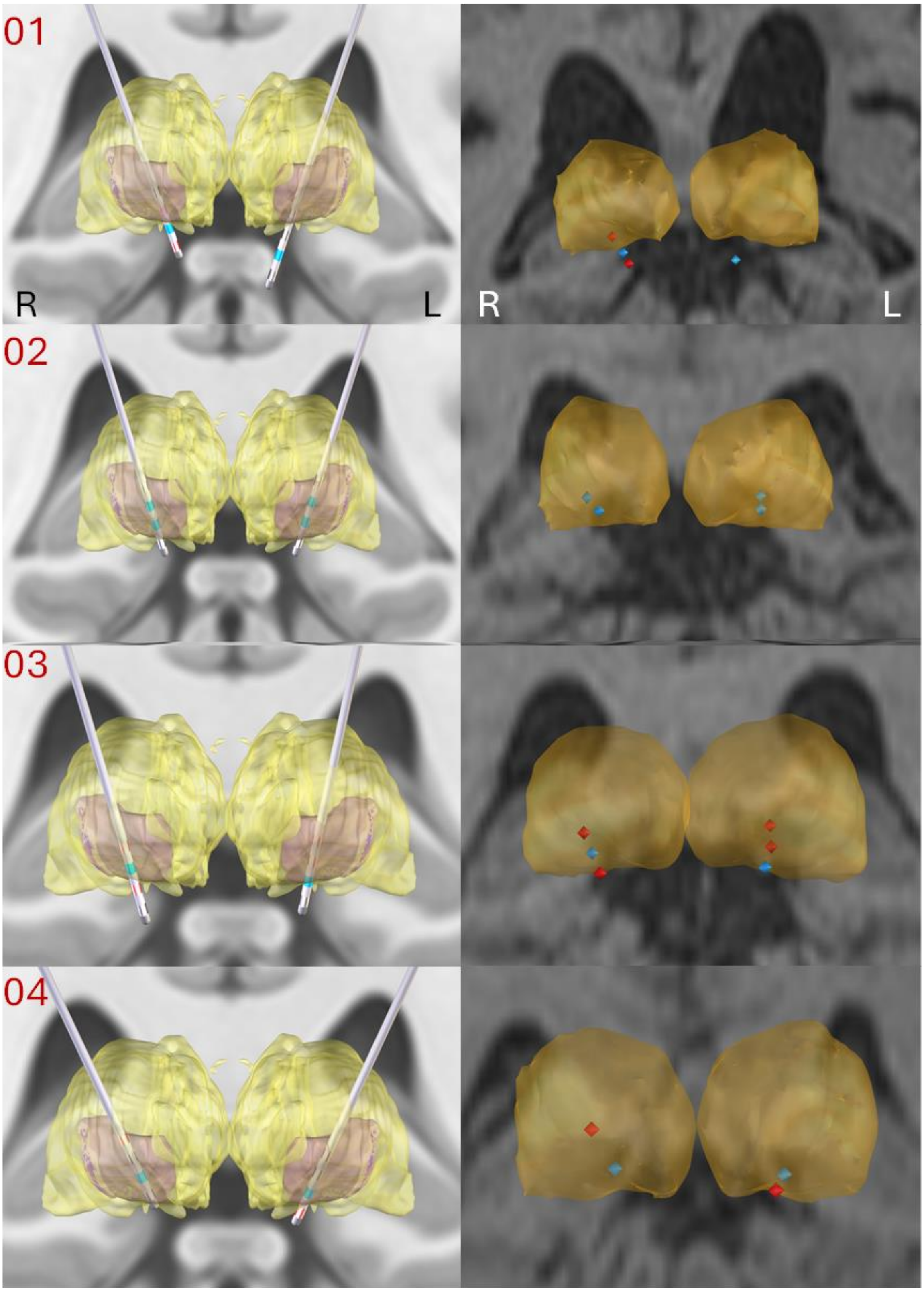

Figure S5

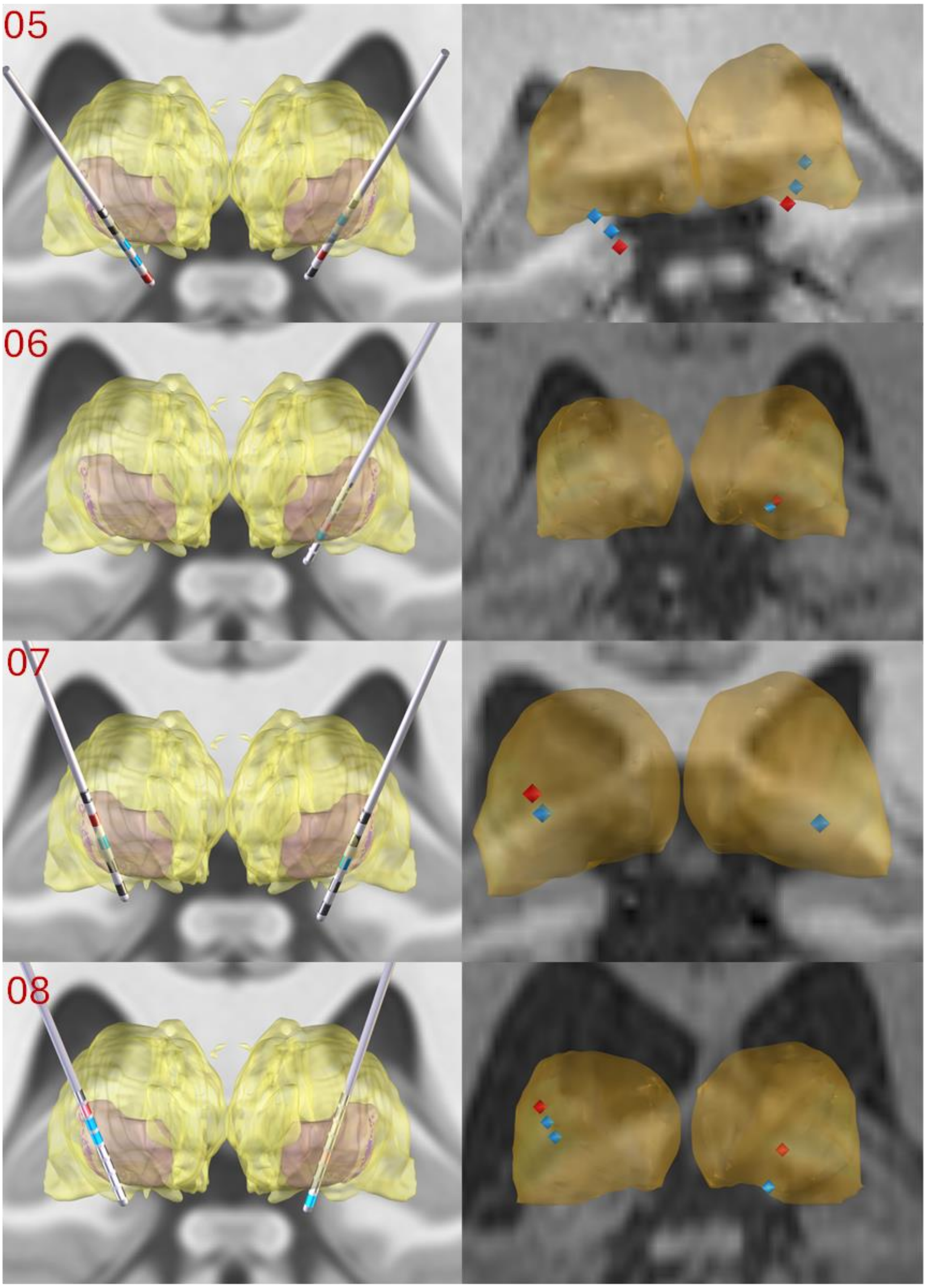
05
06
07
08

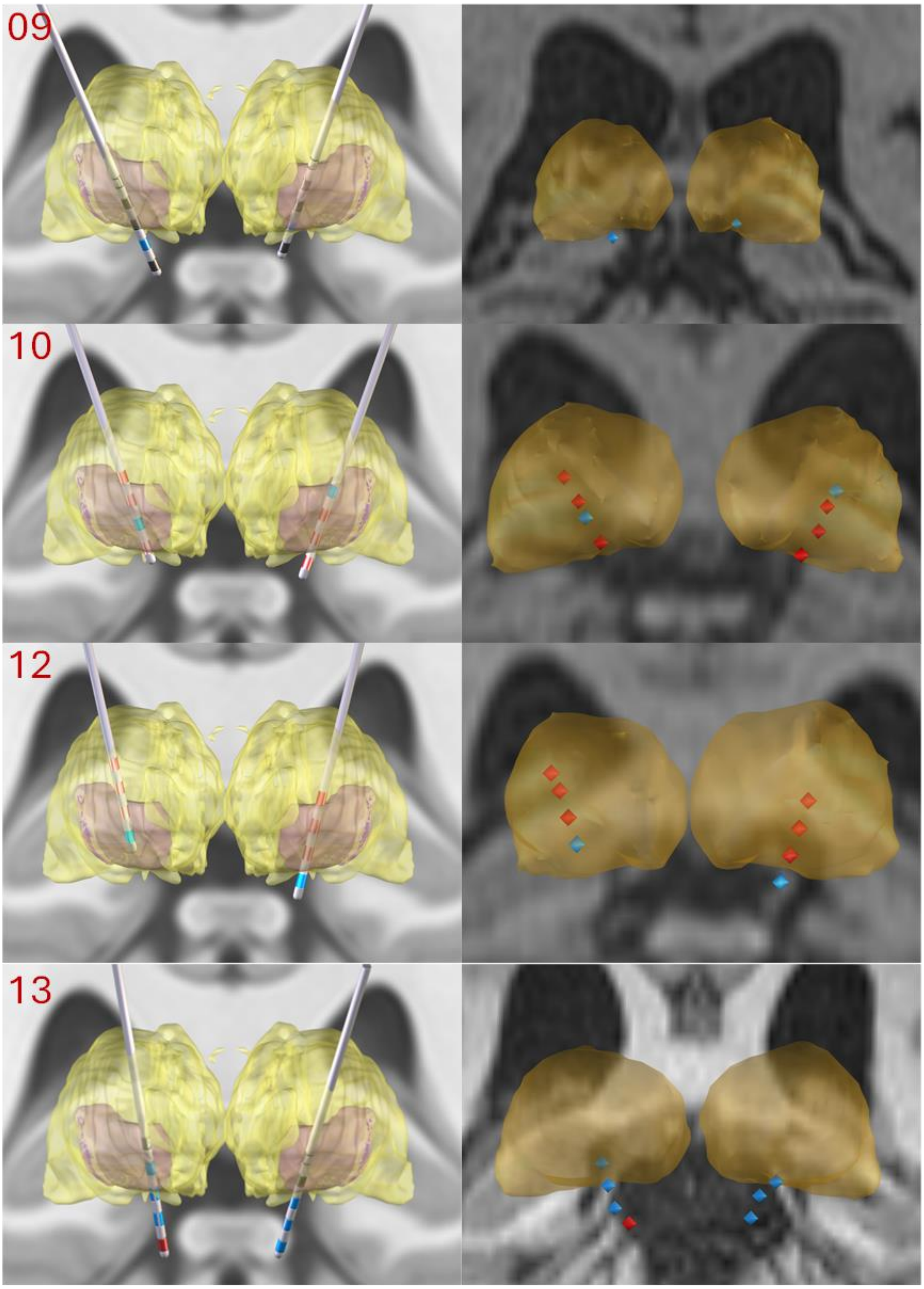
09
10
12
13

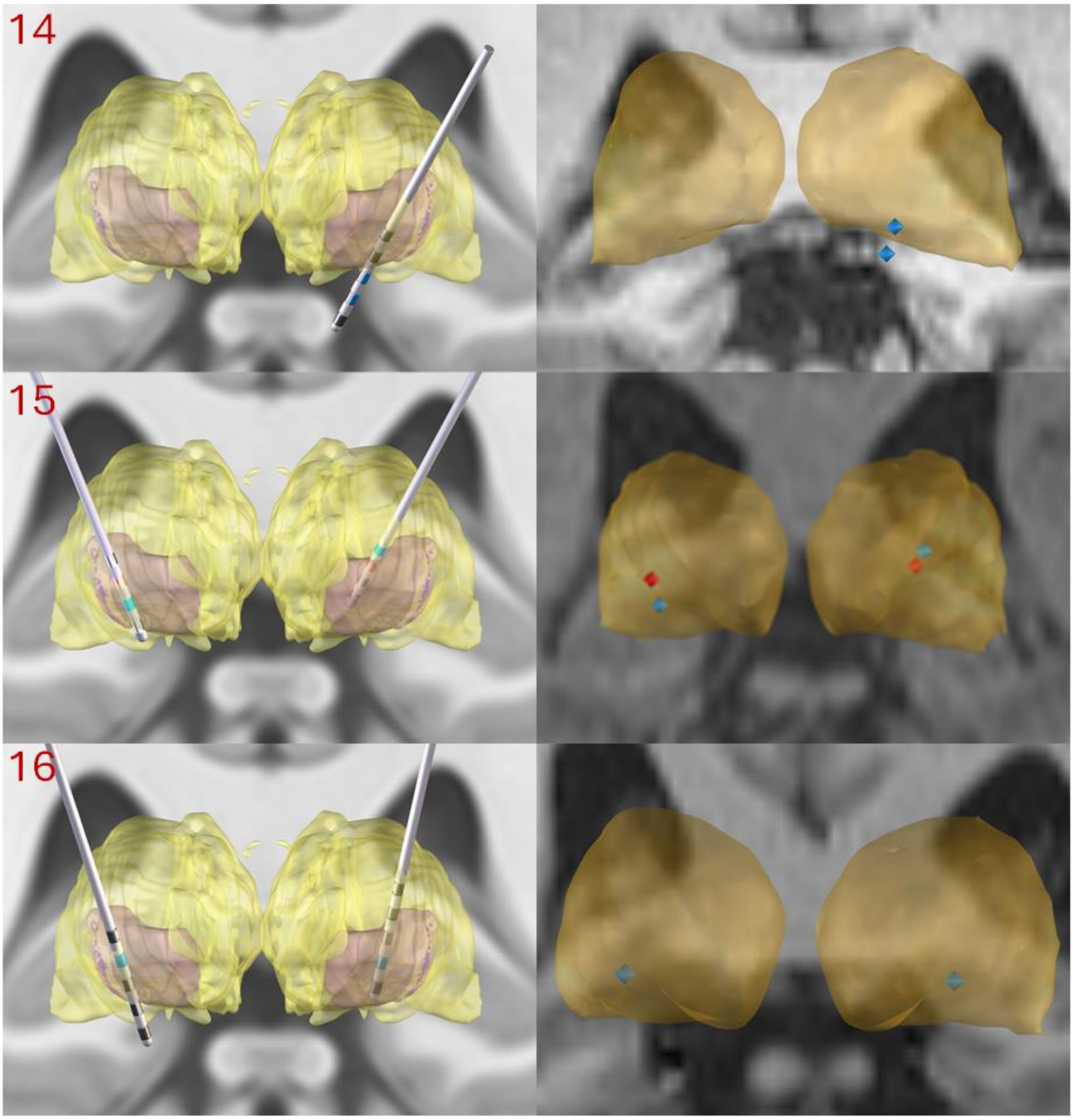
14
15
16

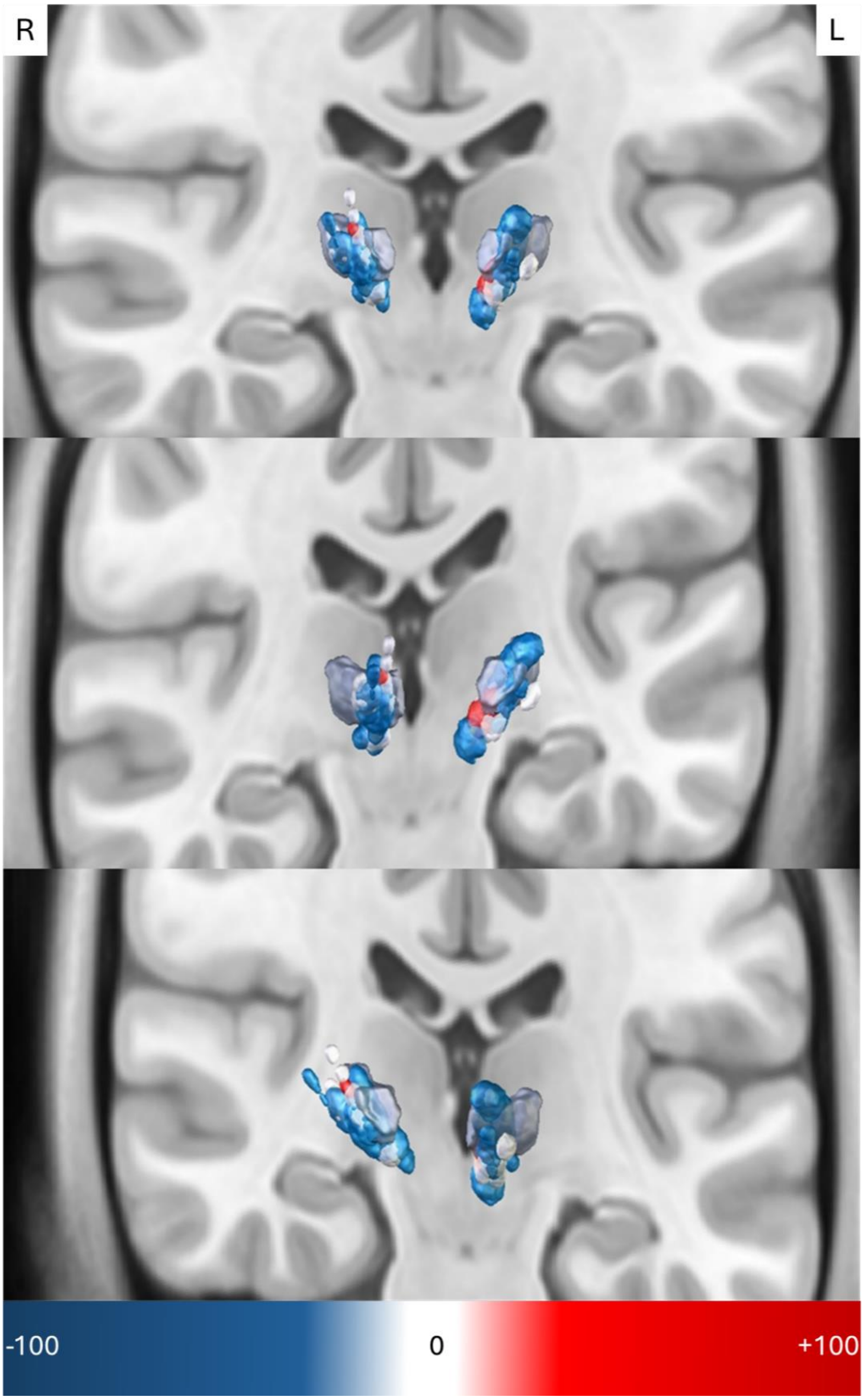

Figure S6